

# Alternative Splicing of Fibroblast Growth Factor Receptor 3 Produces a Secreted Isoform That Inhibits Fibroblast Growth Factor–Induced Proliferation and Is Repressed in Urothelial Carcinoma Cell Lines

Darren C. Tomlinson, Corine G. L'Hôte, Wendy Kennedy, Eva Pitt, and Margaret A. Knowles

Cancer Research UK Clinical Centre, St. James's University Hospital, Leeds, United Kingdom

## Abstract

**Fibroblast growth factor receptors (FGFRs) are a family of receptor tyrosine kinases that play key roles in proliferation, differentiation, and tumorigenesis. FGFR3 was identified as the major family member expressed in both normal human urothelium and cultured normal human urothelial (NHU) cells and was expressed as the IIIb isoform. We also identified a splice variant, FGFR3  $\Delta$ 8-10, lacking exons encoding the COOH-terminal half of immunoglobulin-like domain III and the transmembrane domain. Previous reports have assumed that this is a cancer-specific splice variant. We showed that FGFR3  $\Delta$ 8-10 is a normal transcript in NHU cells and is translated, N-glycosylated, and secreted. Primary urothelium expressed high levels of FGFR3 transcripts. In culture, levels were reduced in actively proliferating cells but increased at confluence and as cells approached senescence. Cells over-expressing FGFR3 IIIb showed FGF1-induced proliferation, which was inhibited by the addition of FGFR3  $\Delta$ 8-10. In bladder tumor cell lines derived from aggressive carcinomas, there were significant alterations in the relative expression of isoforms including an overall decrease in the proportion of FGFR3  $\Delta$ 8-10 and predominant expression of FGFR3 IIIc in some cases. In summary, alternative splicing of FGFR3 IIIb in NHU cells represents a normal mechanism to generate a transcript that regulates proliferation and in bladder cancer, the ratio of FGFR3 isoforms is significantly altered.** (Cancer Res 2005; 65(22): 10441-9)

## Introduction

Fibroblast growth factor (FGF) receptors (FGFRs) play important roles in many biological processes ranging from skeletal development to carcinogenesis. The FGFR family consists of four main members (FGFR1-4) of high-affinity cell surface-associated receptors, which are highly conserved both within the family and throughout evolution (1). FGFR1 to 4 have a core structure, which consists of an extracellular domain that includes an NH<sub>2</sub>-terminal hydrophobic signal peptide followed by three immunoglobulin (Ig)-like domains, a hydrophobic transmembrane domain, and an intracellular tyrosine kinase domain. FGFs, the ligands for FGFRs, bind to the extracellular Ig-like domains II and III (2), resulting in downstream signaling. Specificity of FGF binding is conferred not

only by the receptor family member but also by alternative splicing of FGFRs (3). For example, the COOH-terminal half of Ig domain III may be encoded by either of two exons, resulting in a IIIb or IIIc isoform (refs. 1, 4, 5; Fig. 3A). The receptors and their isoforms are expressed in a cell- and tissue-specific manner, which is necessary for their differential roles in different tissues and cell lineages. Inappropriate expression or mutation of these receptors is involved in both malignant diseases (6–10) and skeletal dysplasia syndromes (11). Missense mutations in the extracellular and intracellular regions of the receptor may result in receptor activation (12) or defective receptor degradation (13).

Several autosomal dominant heritable disorders of skeletal development are caused by missense mutations in *FGFR1*, 2, and 3, which lead to constitutive activation of the kinase activity of the receptors (14). Consistent with the phenotype of these skeletal disorders in humans, constitutive activation of FGFR3 in mouse models causes impaired long bone growth and differentiation (15). Mutations of *FGFR3* identical to those found in skeletal dysplasia syndromes have been identified recently in multiple myeloma (16), bladder carcinoma (8, 17, 18), cervical carcinoma (8), and benign skin tumors (19). In multiple myeloma, 25% of cases show a t(4;14)(p16;q32) that translocates *FGFR3* on chromosome 4 into the *IgH* locus on chromosome 14, resulting, in some cases, in overexpression of wild-type FGFR3 from the derivative 14. *FGFR3* mutations in the fusion protein are infrequent but have been associated with tumor progression (16). A large proportion of urothelial cell carcinomas of the bladder (>40% overall) show mutation of *FGFR3* with a clear association of mutation with low tumor grade and stage (17, 20).

In addition to constitutive activation of FGFR3 in certain tumors, distinct mRNA splice variants have been identified in a range of tissues and cancers. Chellaiah et al. (5) described the first splice variant of FGFR3, FGFR3 IIIb. Later, reverse transcriptase-PCR (RT-PCR) analysis of FGFR3 in a breast epithelial tumor cell line (MCF-7) showed the presence of another splice variant in which exons 9 and 10 (originally described as exons 7 and 8) were deleted (21). The same isoform was also identified in the human osteosarcoma cell line SaOS-2 and the squamous carcinoma cell line DJM-1 and was shown to be soluble and capable of binding both FGF1 and FGF2 (22, 23). Numerous other isoforms have been identified, some of which result in frameshifts and premature termination in exon 10 (24) and others, with deleted domains, which remain in-frame (25, 26). Characterization of these variants has led to the suggestion that aberrant splicing of FGFR3 mRNA may result in a selective advantage for cancer cells (24–26).

As mutational activation of FGFR3 clearly plays a major role in the development of bladder cancer, it is important to understand the role of FGFRs in urothelial cells. Here, we aimed to characterize

**Requests for reprints:** Margaret A. Knowles, Cancer Research UK Clinical Centre, St. James's University Hospital, Beckett Street, Leeds LS97TF, United Kingdom. Phone: 44-11-3206-4913; Fax: 44-11-3242-9886; E-mail: margaret.knowles@cancer.org.uk.

©2005 American Association for Cancer Research.  
doi:10.1158/0008-5472.CAN-05-1718

the expression of FGFRs and particularly FGFR3 isoforms in normal and tumor-derived human urothelial cells. Real-time quantitative RT-PCR was used to measure levels of FGFR mRNA in cultured normal human urothelial (NHU) cells and primary uncultured urothelial cells. This showed that FGFR3 is the most abundantly expressed FGFR in this cell type. RT-PCR and sequencing were done to identify the different mRNA isoforms of FGFR3 expressed. The mRNA isoforms were quantified by real-time RT-PCR throughout the NHU life span *in vitro* and the most abundant isoforms (FGFR3 IIIb and FGFR3  $\Delta$ 8-10) were cloned and characterized in NHU cells. Finally, we analyzed the expression of FGFR3 splice variants in urothelial cell carcinoma cell lines.

## Materials and Methods

**Cell lines.** Primary NHU cells were derived from urothelium stripped from human ureters obtained at nephrectomy from patients with renal carcinoma (three male and five female; age range, 50-86 years; average age, 67 years). In all cases, the renal carcinoma was confined to the kidney and the ureters were histologically normal. Cells were derived as described (27) and maintained in KSFM keratinocyte medium (Life Technologies, Inc., Paisley, Scotland, United Kingdom) supplemented with epidermal growth factor and bovine pituitary extract (Invitrogen, Paisley, Scotland, United Kingdom). For expressing and characterizing FGFR3 constructs, telomerase-immortalized NHU cells (NHU-TERT) were used. Twenty-two bladder cancer cell lines were used: 97-7, RT4, RT112M, 97-18, 94-10, 97-6, BFTC905, 97-29, SCaBER, DSH1, VMCUB3, SW1710, 96-1, VMCUB2, 97-24, J82, HT1376, 97-1, 647V, 253J, BFTC909, and 5637. Cell lines were grown in standard media at 37°C in 5% CO<sub>2</sub>.

**Detection of fibroblast growth factor receptor 3 splice variants by reverse transcription-PCR.** Total cellular RNA was extracted using Qiagen RNeasy Mini Kit (Qiagen, Crawley, West Sussex, United Kingdom) and 1 µg was reverse transcribed in the presence or absence of reverse transcriptase (Advantage RT-for-PCR kit, Clontech, Cowley, Oxfordshire, United Kingdom) according to the instructions of the manufacturer. Primer sequences were chosen within exons 6, 8, 9, and 11 (exon 6-forward, 5'-aactacacctcgctgtggag-3'; exon 8-reverse, 5'-ggcctccactctcactgac-3'; exon 9-reverse, 5'-tagctcctgtcgggtggttag-3'; exon 11-reverse, 5'-agctcgagctcgagcattg-3'). Thirty-five cycles of PCR were done: 95°C for 1 minute, then 35 cycles of 94°C for 30 seconds, 60°C for 30 seconds, and 72°C for 45 seconds. PCR products were visualized by agarose gel (2%) electrophoresis and ethidium bromide staining. Products were sequenced using the ABI PRISM Big dye terminator kit V1.1 (Perkin-Elmer, Applied Biosystems, Warrington, Cheshire, United Kingdom) on an ABI 3100 Genetic Analyser.

**Quantitative real-time reverse transcriptase-PCR.** Real-time RT-PCR analysis was done using SYBR Green I as reporter and ROX as reference dye (Applied Biosystems). FGFR primers were designed to span exons (FGFR1-forward, 5'-aggctacaaggtccggttatgc-3'; FGFR1-reverse, 5'-tgcctactcattctccacaa-3'; FGFR2-forward, 5'-ttaagcaggagcattgac-3'; FGFR2-reverse, 5'-gggacacactttcataatgag-3'; FGFR3-forward, 5'-cctcgggagatgacgaagac-3'; FGFR3-reverse, 5'-cgggcccgtgtccagtaagg-3'; FGFR4-forward, 5'-tgcagaatctcacttgatataca-3'; FGFR4-reverse, 5'-ggggtaactgtgcctattcg-3'). Primer pairs were assessed for PCR efficiency from a standard curve derived from reactions using serially diluted cDNA and compared with two control genes [hypoxanthine phosphoribosyltransferase (*HPRT*): *HPRT*-forward, 5'-gacactggcaaaacaatgca-3'; *HPRT*-reverse, 5'-cttctgtgggtcttttacc-3'; succinate dehydrogenase subunit A (*SDHA*): *SDHA*-forward, 5'-tgggaacaagggcactctg-3'; *SDHA*-reverse, 5'-ccaccactgcatcaaatcatg-3']. Cycle parameters were: initialization at 50°C for 2 minutes, incubation at 95°C for 10 minutes, followed by 40 cycles of 95°C for 15 seconds, 60°C for 1 minute, and finally 95°C for 15 seconds. Melting curve analysis [temperature ramp from 60°C (20 seconds) to 95°C (15 seconds) at 0.029°C/s] was used to ensure the presence of only one PCR product. PCR reactions and analyses were done on the ABI PRISM 7700 Sequence Detector. RNA and template-free controls were included.

FGFR3 isoform levels were analyzed with the following primers: exon 7-forward, 5'-gagttccactgcaaggtgtacagt-3'; exon 8-forward, 5'-caaagctcggat-

cagtggagat-3'; exon 9-reverse, 5'-gagagaaccttagctctgtgag-3'; exon 10-reverse, 5'-aggaagaagcccaccg-3'; exon 11-reverse, 5'-tcatggacgctgtggact-3'. Primers for each isoform were exon 8-forward and exon 10-reverse (FGFR3 IIIb); exon 7-forward and exon 9-reverse (FGFR3 IIIc); exon 7-forward and exon 11-reverse (FGFR3  $\Delta$ 8-10).

**Western blotting and immunoprecipitation.** Cells were lysed in RIPAE buffer [1% Triton X-100, 1 mmol/L EDTA, 0.1% SDS, 0.5% sodium deoxycholate, 10% glycerol, and protease inhibitor cocktail (Sigma, Poole, Dorset, United Kingdom) in PBS] and lysates cleared by centrifugation at 10,000 rpm at 4°C. Protein concentrations were determined using the bicinchoninic acid assay (Pierce, Woburn, MA). Cell lysates were N-deglycosylated following denaturation of proteins at 96°C for 5 minutes using 5 units of PNGase (Sigma) in 500 µL of lysate and incubation at 37°C for 8 hours.

Medium was conditioned for 3 days, filtered using a 0.2-µm filter, and concentrated using Macrosep concentrators (Pall, Portsmouth Hampshire, United Kingdom). Immunoprecipitation of FGFR3 was carried out using lysate or medium mixed with an FGFR3 antibody and protein A-Sepharose beads (Amersham Biosciences, Little Chalfont, Buckinghamshire, United Kingdom). Antibodies recognizing the cytoplasmic (C; Sigma), extracellular (E; Sigma), and IIIb or IIIc (R&D Systems, Abingdon, Oxfordshire, United Kingdom) domains were used. Proteins were visualized by Western blotting using anti-FGFR3 antibody B9 (Autogen Bioclear, Calne, Wiltshire, United Kingdom) or FLAG antibody (Sigma) with chemiluminescence (ECL Plus Kit, Amersham Biosciences). Blots were stripped in 50 mmol/L Tris (pH 7.5), 10 mol/L urea at 55°C for 1 hour before reprobing with anti- $\alpha$ -tubulin for use as a loading control.

**Cloning and expression of fibroblast growth factor receptor 3 and fibroblast growth factor receptor 3 isoform  $\Delta$ 8-10.** FGFR3 and FGFR3  $\Delta$ 8-10 were cloned into a retroviral expression vector (pFB-neo; Stratagene, La Jolla, CA) modified to contain a hygromycin resistance cassette and either a FLAG (pFB-FLAG-Hyg) or 6 $\times$  His tag (pFB-His-Hyg). Cell lines had been previously transduced with the ecotropic retroviral receptor to allow ecotropic transduction.

FGFR3 was amplified by PCR from pcDNA3 containing FGFR3 IIIb cDNA (kind gift from Dr. D. Podolsky, Harvard Medical School, Boston, MA) to remove the translation stop codon. PCR products were ligated into pGEM-T-Easy vector, inserts were verified by sequencing and subcloned into pFB-FLAG-Hyg. FGFR3  $\Delta$ 8-10 was amplified by PCR from NHU cDNA, ligated into pGEM-T-Easy vector, and subcloned into pFB-FLAG-Hyg.

**Production of retroviruses and infections.** FGFR3 constructs were transfected into the PhoenixE packaging cell line (ATCC). After 48 hours, medium was harvested, 0.4-µm filtered, and mixed in equal amounts with fresh growth medium containing 8 µg/mL of polybrene (Sigma). NHU-TERT cells were grown to 50% confluence and then incubated with retroviral supernatants overnight at 37°C. Forty-eight hours after infection, cells were transferred into selection medium containing hygromycin.

**Purification of His-tagged protein.** NHU-TERT cells were transduced with pFB-FGFR3  $\Delta$ 8-10-His and selected with hygromycin. FGFR3  $\Delta$ 8-10-His was purified from cell lysates using Qiagen Ni-NTA magnetic agarose beads according to the instructions of the manufacturer.

**Cross-linking of fibroblast growth factor receptor 3 isoform  $\Delta$ 8-10.** Cells were washed twice in ice-cold PBS and then incubated at room temperature in the presence of 1 mmol/L disuccinimidyl suberate solution (Sigma). The reaction was terminated by the addition of 1 mol/L Tris to a final concentration of 10 to 20 mmol/L. Cells were washed in PBS, lysed with RIPAE buffer, and analyzed by Western blot as described above.

## Results

**Fibroblast growth factor receptor 3 is the predominant fibroblast growth factor receptor expressed in normal urothelium.** Previous studies have examined levels of FGFRs in bladder cancer but have not examined expression levels in normal cells. We used real-time RT-PCR to examine expression levels of all FGFR family members. Levels of receptors were initially examined in primary urothelium (Fig. 1A). FGFR3 was the most abundantly

expressed receptor and FGFR1, FGFR2, and FGFR4 were all expressed at low levels, indicating that FGFR3 might be the dominant FGFR in normal urothelium. Next, we asked whether primary NHU cells in culture retained the levels of FGFRs observed in primary uncultured urothelial cells (Fig. 1B). Some variability was observed between samples ( $n = 6$ ) but, on average, FGFR3 mRNA levels were highest (26-fold higher than FGFR1). FGFR2 was also highly expressed (14.5-fold higher than FGFR1) and FGFR4 and FGFR1 were least abundant. This suggests that FGFR2 may play an important role in NHU cells in culture. However, NHU cells retained the high level of expression of FGFR3 transcripts seen in uncultured primary cells.

**Passage number and confluence affect the relative levels of fibroblast growth factor receptor 3 isoforms.** Total levels of FGFR3 mRNA varied between NHU samples and we confirmed that this variability was also observed at the protein level between NHU cell strains (Fig. 2A). The NHU cell strain with the highest mRNA level also expressed the most protein and vice versa. To determine if this variability was due to cell density or donor variation, we compared FGFR3 levels in primary and cultured cells from the same donor, from initial plating until senescence. We observed a significant decrease in FGFR3 mRNA levels after initial plating (Fig. 2B). Levels also differed between proliferating cells

and confluent cells at the same passage. At passage 1, confluent cells expressed 2.5-fold less FGFR3 mRNA than proliferating cells. Between passages 2 and 7, levels were 6- to 50-fold higher in confluent cells than in proliferating cells. Confluent cells at passage 7 expressed very similar total FGFR3 mRNA levels to primary uncultured cells. The difference at passage 1 compared with passages 2 to 7 may be due to adaptation to culture conditions.

**Presence of multiple fibroblast growth factor receptor 3 isoforms in normal urothelial cells.** Novel FGFR3 mRNA isoforms have been identified in some cancer cells but few studies have examined normal cells of any type and none have examined urothelial cells. RT-PCR was done on NHU cDNA with primers spanning the third Ig-like loop of the extracellular domain and the transmembrane domain (from exons 6 to 11; Fig. 3A, arrows). This generated nine PCR products (Fig. 3B). Five products were successfully sequenced: an 855-bp sequence encompassing exons 6 to 11, which results in a premature translation termination; a 710-bp sequence that represented FGFR3 IIIb; a 559-bp sequence encompassing exons 6, 7, 10, and 11, which results in a premature translation termination; a 519-bp sequence encompassing exons 6, 7, 8 and 11, which results in premature translation termination; and a 368-bp sequence encompassing exons 6, 7, and 11, which does not result in premature translation termination (Fig. 3E). Translation of this latter splice variant (FGFR3  $\Delta$ 8-10) would result in an FGFR3 protein missing the second part of the third Ig-like loop and the transmembrane domain. All of the splice variants lacking exon 10 occasionally retained 3 bp from exon 10 (Fig. 3E, *underlined CAG*). Primers were designed in the alternatively spliced exons for FGFR3 IIIb and IIIc, exons 8 and 9, respectively (Fig. 3A). RT-PCR was done using reverse primers in exon 8 or 9 with the forward primer in exon 6 on two NHU cell strains. The resulting PCR products are shown in Fig. 3C. Only the IIIb isoform was amplified using primers in exons 6 and 8 (Fig. 3C, a), which was confirmed by sequencing. Two bands were observed in the PCR product using primers in exons 6 and 9 (Fig. 3C, b and c), which were sequenced and confirmed to be the unspliced product (exons 6-11) and FGFR3 IIIc. The unspliced product was identified as a low abundance product using primers in exons 6 and 11 (Fig. 3B, *top arrow*), yet it seemed to be more abundant than the IIIc isoform. This suggested that the IIIc isoform is expressed in NHU cells at very low levels. It has also been reported that exon 4 can be spliced, resulting in an FGFR3 protein missing the acid box (26). RT-PCR showed no deletion of this region in any normal or cancer cell line examined (data not shown).

**Fibroblast growth factor receptor 3 isoform  $\Delta$ 8-10 is a major fibroblast growth factor receptor 3 transcript in normal cells.** The amplified PCR products shown in Fig. 3B suggested that FGFR3  $\Delta$ 8-10 is the most abundantly expressed FGFR3 isoform in NHU cells. Real-time RT-PCR was used to examine levels of FGFR3 isoforms in NHU cell strains and primary uncultured urothelial cells (Fig. 3D). The uncultured primary cells contained mainly FGFR3 IIIb but small amounts of FGFR3 IIIc and FGFR3  $\Delta$ 8-10 were also present. Such cells are quiescent in the normal ureter. To confirm that expression of FGFR3  $\Delta$ 8-10 was not an artifact of cell culture but was associated with urothelial proliferation both *in vivo* and *in vitro*, we carried out RT-PCR using primers in exons 6 and 11 on RNA derived from a low-grade noninvasive bladder tumor. We found that FGFR3  $\Delta$ 8-10 was expressed. NHU cells in culture expressed both FGFR3 IIIb and FGFR3  $\Delta$ 8-10 and the relative amount of FGFR3  $\Delta$ 8-10 increased at confluence in late-passage cells. This suggests that FGFR3  $\Delta$ 8-10 is involved in the regulation

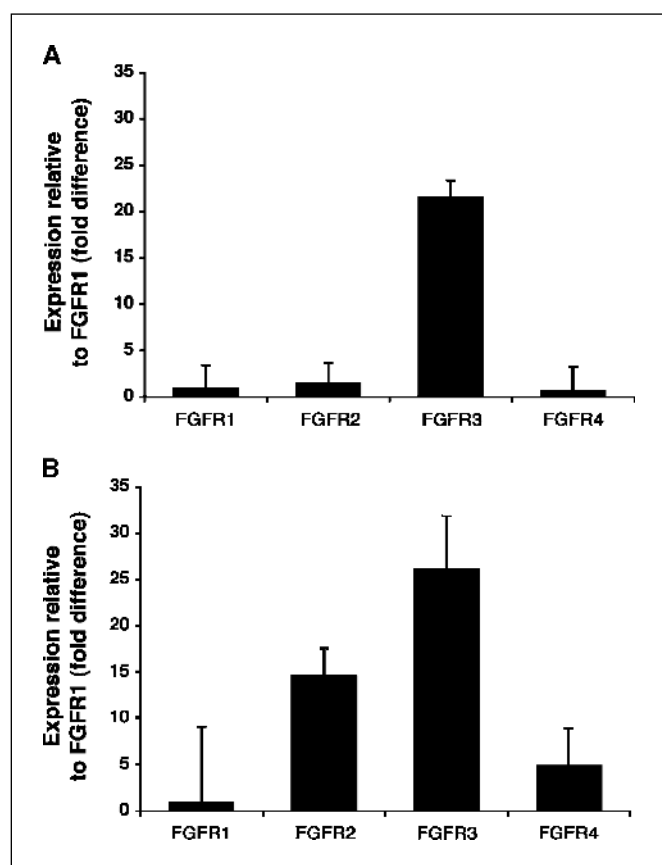


**Figure 1.** Expression of FGFR levels in NHU cells and uncultured urothelium. FGFR mRNA levels were measured by real-time PCR and normalized to either HPRT or SDHA. Values represent fold difference compared with FGFR1 mRNA levels. A, differences in FGFR mRNA levels (average of three uncultured urothelial samples). FGFR3 was the most highly expressed family member. B, differences in FGFR mRNA levels in NHU cells (average from six NHU cell strains). Bars, SE.



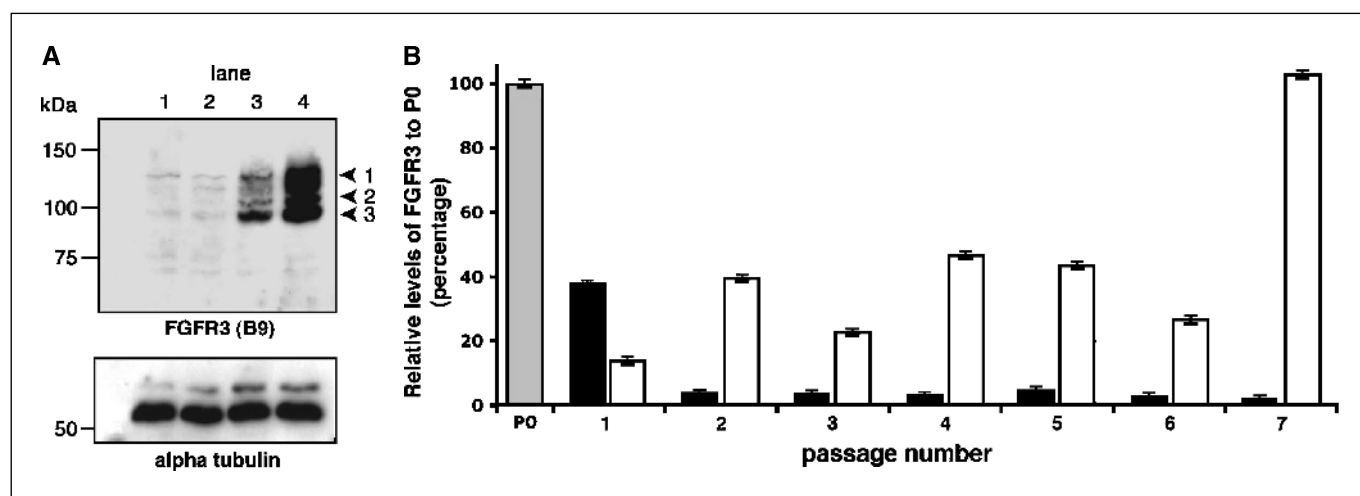


**Figure 2.** Expression analysis of FGFR3 protein and mRNA in NHU cells. *A*, the blot was probed with the anti-FGFR3 B9 antibody. Lanes 1 to 4, different NHU strains. Arrows, three main bands detected. Band 1 consists of two or three indistinguishable bands. Anti- $\alpha$ -tubulin antibody was used as a control for protein loading. *B*, FGFR3 mRNA levels in cultured urothelial cells at low and high confluence from passage 1 to passage 7. Levels of FGFR3 mRNA represented as a percentage of passage 0 (primary uncultured; P0) FGFR3 mRNA levels. ■, subconfluent; □, confluent; ◻, uncultured urothelium; bars, SD.

of cell proliferation as FGFR3  $\Delta$ 8-10 is expressed in proliferating cells in culture but not in primary (quiescent) cells.

**Fibroblast growth factor receptor 3 isoform  $\Delta$ 8-10 is translated, glycosylated, and secreted.** Immunoprecipitation using antibodies that recognize different regions of FGFR3 was employed to identify the protein band that represents FGFR3  $\Delta$ 8-10 on a Western blot. This was possible as antibody E recognizes an epitope encoded by exon 10, which is absent in the FGFR3  $\Delta$ 8-10 isoform (Fig. 4A). Immunoprecipitation using antibody C, which recognizes the COOH-terminal domain, was used as a control (Fig. 4B) and showed a similar pattern of protein bands to that observed by Western blotting of other NHU cell lysates (Fig. 2A). However, when the lysates were immunoprecipitated with antibody E, band 3 disappeared, suggesting that this represented FGFR3  $\Delta$ 8-10. The predicted molecular weights for FGFR3 IIIb and FGFR3  $\Delta$ 8-10 are 88 and 76 kDa, respectively. The presence of larger protein bands on the Western blots suggests that FGFR3 isoforms undergo posttranslational modification. To confirm that band 3 represents a posttranslationally glycosylated FGFR3  $\Delta$ 8-10 protein, the immunoprecipitation was repeated using protein lysates treated with the N-deglycosylation enzyme PNGaseF. Deglycosylation of the protein resulted in two bands (Fig. 4B) that were approximately the predicted molecular weights. Once again, FGFR3  $\Delta$ 8-10 (band 5) was not immunoprecipitated by antibody E. In addition, the levels of the  $\Delta$ 8-10 isoform protein seemed to be similar to the mRNA levels measured by real-time PCR.

Recent reports have shown that FGFR3  $\Delta$ 8-10 is secreted into the culture medium (22, 23). To show this effect in NHU cells, we characterized the expression of FGFR3  $\Delta$ 8-10 in NHU-TERT cells<sup>1</sup> transduced with pFB-FGFR3  $\Delta$ 8-10-FLAG-Hyg (a retroviral expression vector). These cells expressed FGFR3  $\Delta$ 8-10 both intra- and extracellularly (Fig. 4C, lanes 3 and 6). Immunoprecipitation using antibodies C (lane 8) and IIIb (lane 10) confirmed that the protein observed in the medium was FGFR3  $\Delta$ 8-10. This was not detected in NHU-TERT cells transduced with empty vector or pFB-FGFR3

IIIb-FLAG-Hyg either in cell lysates or conditioned medium (Fig. 4C). However, a protein of about 55 kDa was observed in the medium of cells that expressed FGFR3 IIIb. This band was only detected when medium was immunoprecipitated and blotted with antibodies binding to the extracellular region of FGFR3, suggesting that the extracellular domain of the FGFR3 IIIb was cleaved into the medium. Immunoprecipitation using antibodies C (lane 7) and IIIb (lane 9) confirmed that this protein was the extracellular region of FGFR3.

**Fibroblast growth factor receptor 3 isoform  $\Delta$ 8-10 inhibits fibroblast growth factor 1-induced proliferation.** In response to ligand, wild-type FGFR3 can either stimulate or inhibit cell proliferation depending on cell type (26, 28). FGFR3  $\Delta$ 8-10 has been predicted to act as a dominant-negative regulator of FGFR3 signaling (22, 23) but its function has not yet been fully elucidated. We studied the function of FGFR3 isoforms by expressing them in NHU-TERT cells and analyzing the effect of FGF1 on proliferation rate (Fig. 5). Proliferation of cells containing vector only was slightly stimulated (25% increase,  $P < 0.005$  by Student's *t* test) by the addition of low concentrations of FGF1 (1 ng/mL). Higher concentrations of FGF1 did not stimulate proliferation further ( $P = 0.494$ ), suggesting saturation of endogenous receptor. Expression of FGFR3 IIIb resulted in a small but significant increase (12%,  $P < 0.005$ ) in cell number and the addition of FGF1 further increased cell number (56%), and this showed FGF1 dose dependence. Expression of FGFR3  $\Delta$ 8-10 increased the proliferation rate of NHU-TERT cells compared with controls transduced with vector only (36%,  $P < 0.005$ ) or expressing FGFR3 IIIb (22%,  $P < 0.005$ ). However, this was only observed in supplement-free medium and expression of FGFR3  $\Delta$ 8-10 did not alter the FGF1-induced growth compared with controls.

We hypothesized that the secreted or cleaved FGFR3 isoforms may act in a dominant-negative fashion. To test this, conditioned media from cells expressing FGFR3 IIIb and FGFR3  $\Delta$ 8-10 were concentrated 8 $\times$  and added back to culture medium at a final concentration of 1 $\times$ , with and without FGF1 (1 ng/mL). FGF1-induced proliferation of NHU cells expressing FGFR3 IIIb was significantly inhibited ( $P < 0.005$ ) by this conditioned medium. In contrast, conditioned medium from FGFR3 IIIb-expressing cells

<sup>1</sup> Chapman et al., submitted for publication.

had no effect on FGF1-induced proliferation (Fig. 5B). To confirm that FGFR3 Δ8-10 was inhibiting FGF1-induced growth, FGFR3 Δ8-10 was His×6 tagged, expressed in NHU-TERT cells, and purified. Cell lysates from NHU-TERT were used to control for contaminants purified at the same time as the FGFR3 Δ8-10-His. Cell extracts were separated in SDS-PAGE gels and either stained with Coomassie or transferred to nitrocellulose membranes and Western blotted. This confirmed that FGFR3 Δ8-10 was purified and eluted (data not shown). The FGFR3 Δ8-10 purified protein or control extract was added to cultures in the presence of FGF1. Purified FGFR3 Δ8-10 significantly inhibited FGF1-induced proliferation ( $P < 0.005$ ), suggesting that FGFR3 Δ8-10 is a dominant-negative regulator of FGFR3 signaling (Fig. 5C).

**Fibroblast growth factor receptor 3 isoform Δ8-10 dimerizes in response to endogenous fibroblast growth factors.** FGFR3 Δ8-10 may inhibit FGF1-induced proliferation by sequestering FGF1 before binding to FGFR3. To investigate this possibility, the bladder cancer cell line 5637, which expresses low levels of endogenous FGFR3 but high levels of FGF1 (data not shown), was transduced with either vector only or FGFR3 Δ8-10. Cellular proteins were cross-linked using disuccinimidyl suberate and cell extracts were Western blotted (Fig. 5D). The vector control (lanes 1 and 3) showed that there is no nonspecific binding of the antibody to lysates and cross-linked proteins. Cross-linking resulted in three bands (lane 4). The bottom band represents protein of the same size as in lysate from untreated cells. The second band is ~130 kDa larger than the denatured protein and may represent a protein complex of two FGFR3 Δ8-10 molecules. The larger band at the top of the gel may represent a complex of FGFs, FGFR3 Δ8-10, and heparin-like glycosaminoglycans. This shows that FGFR3 Δ8-10 can form dimers in the presence of FGF and this may be a mechanism by which secreted FGFR3 Δ8-10 inhibits FGF1-induced proliferation.

**Fibroblast growth factor receptor 3 splicing is altered in bladder cancer cell lines.** Levels of FGFR3 mRNA isoforms were examined in bladder cancer cell lines (Fig. 6A). FGFR3 IIIb was expressed in the majority of the cell lines examined but in three cell lines (96-1, SW1710, and 253J), <5% of total FGFR3 transcripts were FGFR3 IIIb. Thirteen cell lines (62%) expressed a lower percentage of FGFR3 Δ8-10 isoform than NHU cells. FGFR3 IIIc was the major FGFR3 isoform expressed in the three cell lines that had a reduced

proportion of FGFR3 IIIb. In fact, FGFR3 IIIc was expressed in 11 cell lines (52%) at a higher percentage of total FGFR3 than in NHU cells. To confirm the validity of using real-time RT-PCR to compare isoform levels, we examined levels of FGFR3 protein isoforms using the cell lines 97-7 and SW1710. 97-7 is a urothelial cell carcinoma cell line that expresses low levels of FGFR3 Δ8-10 mRNA (0.5% of total FGFR3 mRNA levels). 97-7 showed a similar banding pattern of FGFR3 proteins to NHU cells (Fig. 6B, 1, 2, and 3), with band 3

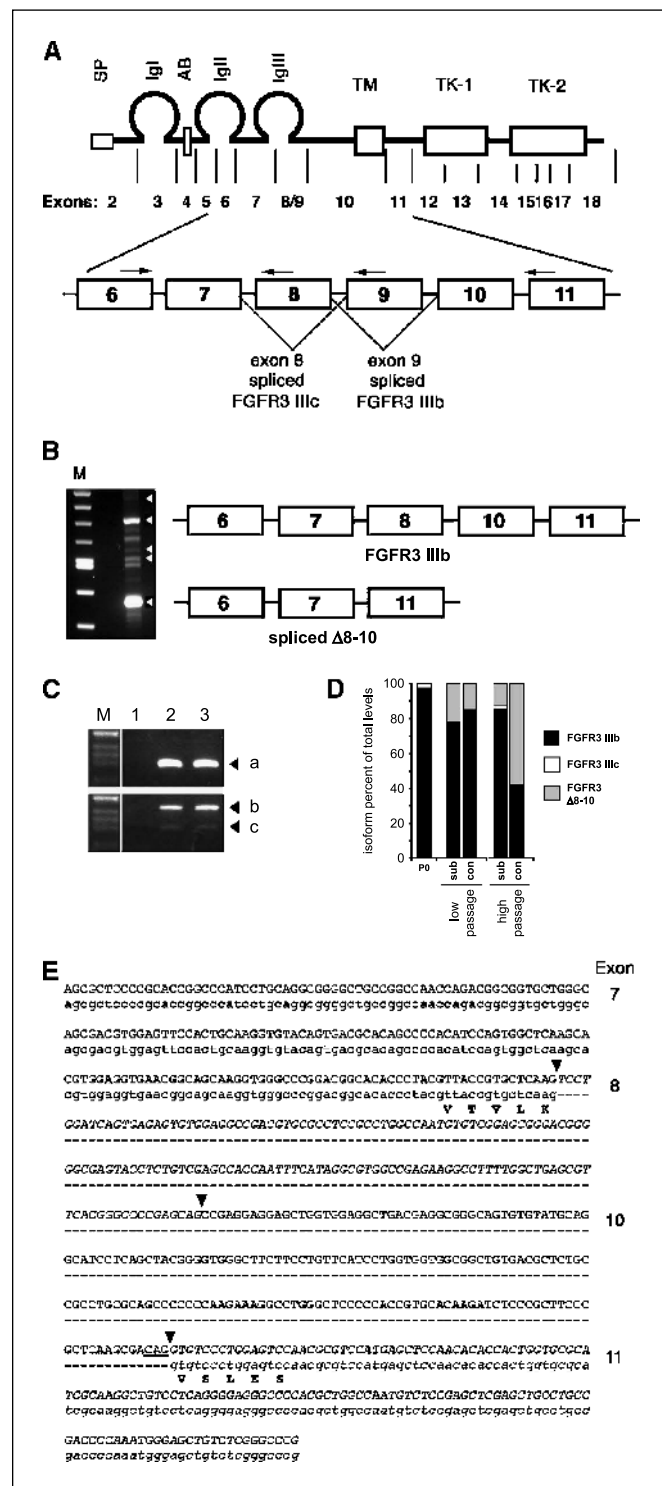


**Figure 3.** Identification and characterization of FGFR3 isoforms. **A**, diagrammatic representation of FGFR3 and the exons that encode each domain. These include the signal peptide (SP), Ig-like domains I, II, and III, the transmembrane domain (TM), and the split tyrosine kinase domain (TK-1 and TK-2). Exons 6 to 11 are magnified to show the normal splicing events that result in either FGFR3 IIIb or FGFR3 IIIc isoforms. The arrows on exons 6, 8, 9, and 11 represent the position of the primers used for PCR to identify the isoforms expressed in bladder cells. **B**, RT-PCR was done on NHU cDNA with primers spanning the third Ig-like loop of the extracellular domain and the transmembrane domain (from exon 6 to 11). PCR products identified by white arrows were characterized by sequencing (other products failed to sequence). **M**, 100-bp DNA ladder (New England Biolabs, Hitchin, Hertfordshire, United Kingdom). **C**, RT-PCR was done using reverse primers in exon 8 or 9 with the forward primer in exon 6. **Lane 1**, RT-negative PCR; **lanes 2 and 3**, PCR products from cDNAs from different NHU cell strains. **Products a, b, and c**, FGFR3 IIIb, unspliced product (exons 6-11), and FGFR3 IIIc, respectively. **M**,  $\phi$ X174 DNA-*Hae*III digest ladder. **D**, FGFR3 isoform levels were measured by real-time RT-PCR in passage 0, subconfluent (*sub*) and confluent (*con*) NHU cells at low and high passage. Levels are represented as a percentage of total FGFR3 levels. **E**, sequence analysis of FGFR3 Δ8-10. **Uppercase letters**, FGFR3 IIIb sequence; **lowercase letters**, FGFR3 Δ8-10 sequence. Exons are labeled on the right; **arrows**, splice sites. **Capital and bold letters**, amino acids; **FGFR3 Δ8-10** remains in frame. **Underlined sequence**, the 3 bp that may or may not be spliced with exon 10.

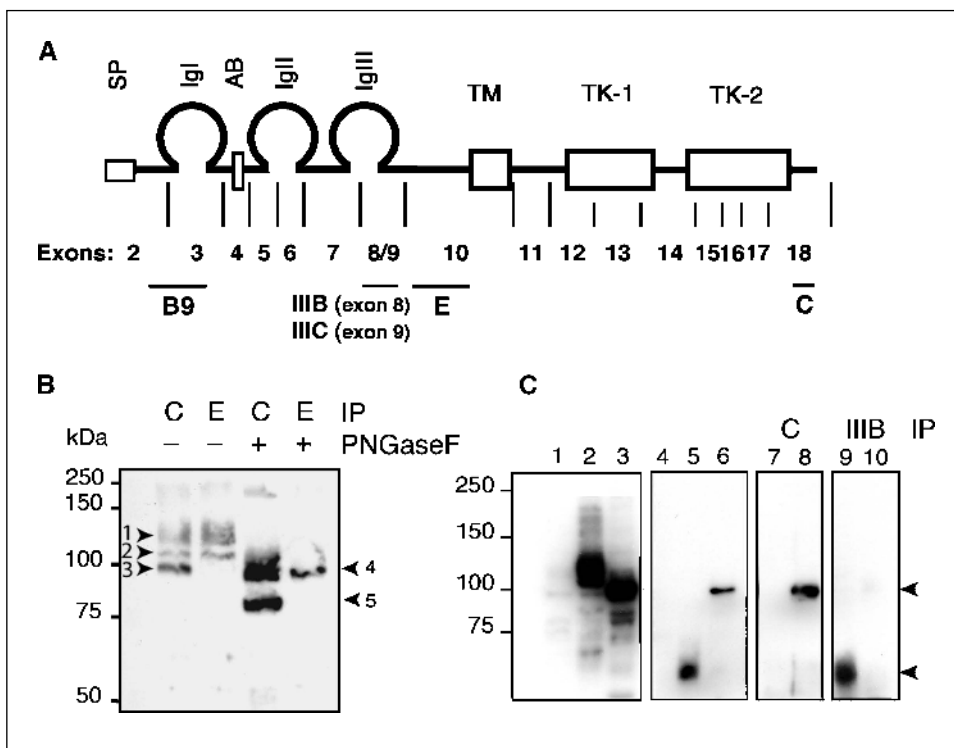


**Figure 4.** Deglycosylation and identification of the presence of FGFR3 isoforms in NHU cell media. *A*, indication of the epitopes recognized by the FGFR3 antibodies: B9 (Autogen Bioclear) against amino acids 25 to 124; E (Sigma) against amino acids 359 to 372; C (Sigma) against amino acids 792 to 806; IIIb and IIIc (R&D Systems) with epitopes in exons 8 and 9, respectively. *Igl* to *IgIII*, immunoglobulin domains; *TM*, transmembrane domain; *TK1* and *TK2*, split tyrosine kinase domain. *B*, lysate from confluent NHU cells at high passage was treated with and without PNGaseF and immunoprecipitated (*IP*) with the anti-FGFR3 C or E antibody. The blot was probed with the B9 antibody. *C*, cell lysate and medium were taken from cells expressing either retroviral vector, FGFR3 IIIb, or FGFR3  $\Delta$ 8-10. Five micrograms of each protein lysate were blotted and probed with the B9 antibody (*lanes 1-3*, respectively). Conditioned medium taken from cells expressing either retroviral vector, FGFR3 IIIb, or FGFR3  $\Delta$ 8-10 was blotted and probed with the B9 antibody (*lanes 4-6*, respectively). Concentrated conditioned medium taken from cells expressing FGFR3 IIIb or FGFR3  $\Delta$ 8-10 was immunoprecipitated with either antibody C (*lanes 7 and 8*) or antibody IIIb (*lanes 9 and 10*). The blot was probed with the B9 antibody.

identified as FGFR3  $\Delta$ 8-10 by immunoprecipitation. Band 3 represents a low percentage of the total FGFR3 protein present, confirming that the mRNA levels measured by real-time RT-PCR bear a direct relationship to the levels of protein expressed. SW1710 expressed FGFR3 IIIc as the major FGFR3 isoform. The expression of FGFR3 IIIc, and not of IIIb or  $\Delta$ 8-10 isoform, at the protein level was confirmed by immunoprecipitation using the IIIc, IIIb, E, and C antibodies and blotting with the B9 antibody (Fig. 6C). The IIIb-specific antibody was the only antibody that did not immunoprecipitate any FGFR3 protein, confirming the altered isoform splicing detected by real-time RT-PCR.

## Discussion

We have shown that FGFR3 is the most abundant FGFR in urothelial cells (Fig. 1), implying that FGFR3 may play an important role in normal urothelial homeostasis. This is compatible with its predicted role as an oncogene involved in the development of the majority of low-grade noninvasive bladder cancers.

Using RT-PCR, a splice variant of FGFR3 missing the second half of the third Ig-like loop and the transmembrane domain has been identified (Fig. 3). Some publications have suggested that alternative splicing of FGFR3 is the result of aberrant splicing mechanisms in cancer cells (23, 24). Interestingly, although levels were not measured in relevant normal controls, one of these studies showed that FGFR3  $\Delta$ 8-10 was expressed at relatively low levels compared with the full-length FGFR3 product in SaOS-2 osteosarcoma cells, which is consistent with our findings in bladder cancer cell lines. Johnston et al. (21) described the same isoform in normal breast epithelial and breast tumor cell lines, with the expression pattern of FGFR3  $\Delta$ 8-10 similar to that observed in our study. The PCR product for FGFR3  $\Delta$ 8-10 was more abundant in normal breast cells (MCF-10A and HBR-SV-161) than in cancer cells (MCF-7). This suggests that FGFR3  $\Delta$ 8-10 is a major transcript in normal cells and is down-regulated in

cancer cells. In fact, we showed that 62% of bladder cancer cell lines expressed a much lower proportion of FGFR3  $\Delta$ 8-10, relative to total transcript levels than any NHU cell strain examined. Our data and that of Johnston et al. (21) suggest that the FGFR3  $\Delta$ 8-10 protein is the result of normal splicing in proliferating cells.

Interestingly, primary uncultured urothelium, which *in vivo* has a very low proliferative index, does not express FGFR3  $\Delta$ 8-10. Our finding of expression of the FGFR3  $\Delta$ 8-10 isoform in cultured urothelium and in uncultured tumor tissue is compatible with the notion that this isoform may be involved in the regulation of FGFR3 signaling in proliferating cells. Alternative splicing was induced as soon as cells began to proliferate shortly after isolation and plating in tissue culture. Our immunoprecipitation and Western blotting analyses confirmed the expression of FGFR3  $\Delta$ 8-10 in cultured cell lysates and showed that its expression was equivalent to that of FGFR3 IIIb. No previous studies have examined primary cells and it will now be interesting to survey a range of normal epithelial tissues for expression of this isoform.

Our data indicate that total FGFR3 expression is reduced during proliferation and increases at confluence in urothelial cells (Fig. 2B). This is opposite to the expression pattern of FGFR1 in the same cells.<sup>2</sup> In proliferating cells, however, overexpression of FGFR3 IIIb can lead to increased proliferation when stimulated in a paracrine fashion by exogenous ligand. These results may indicate different effects of FGFR3 signaling in different growth states of these normal cells, as confluent cells expressing high levels of the receptor cannot exhibit a proliferative response to added ligand. A similar increase in levels of FGFR3 IIIb at confluence has been reported previously in Caco-2 colon cancer cells, which are stimulated by FGF1 when subconfluent but not

<sup>2</sup> Our unpublished data.

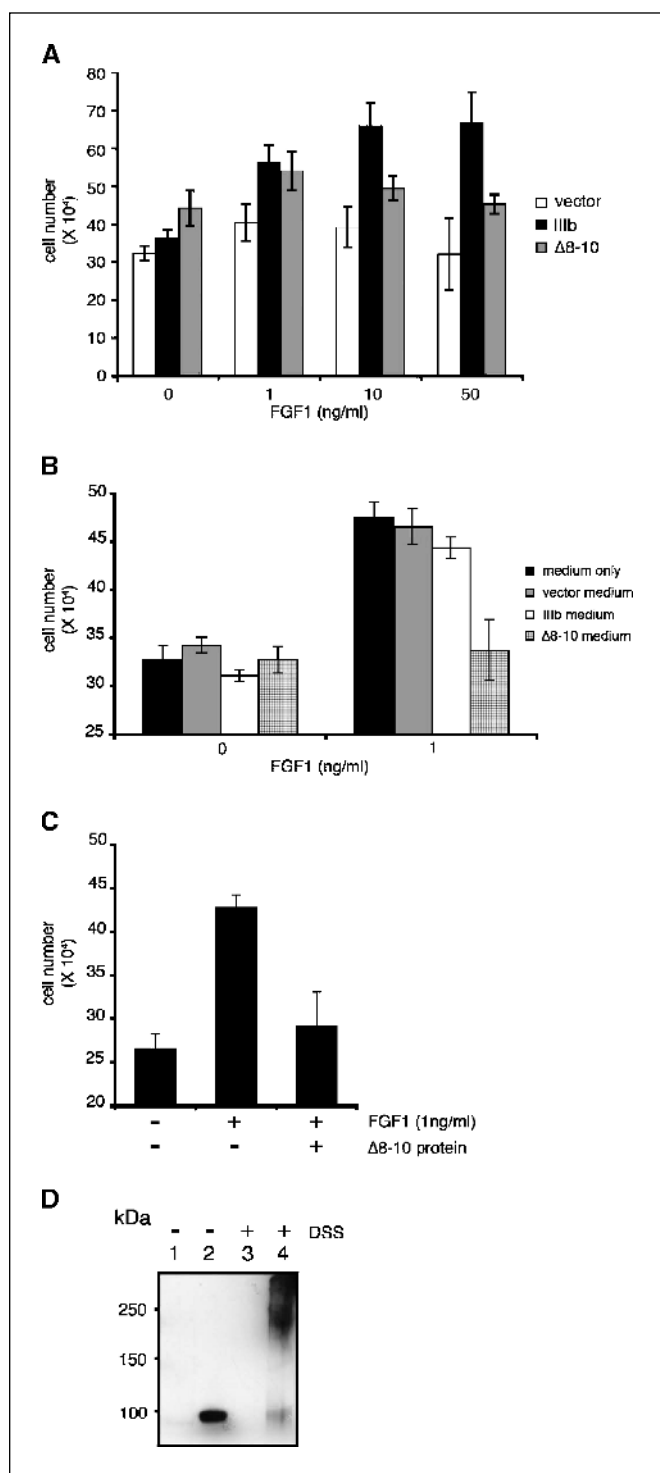


**Figure 5.** A, the effect of FGF1 and overexpression of FGFR3 IIIb and FGFR3 Δ8-10 on cell proliferation. NHU-TERT cells were stably infected with vector (control), FGFR3 IIIb, or FGFR3 Δ8-10 expressing retroviruses. On day 1, cells were incubated with heparin or heparin with either 1, 10, or 50 ng/mL FGF1 in supplement-free medium for 3 days. Each condition was done in triplicate over three independent experiments. Bars, SD. NHU cells expressing FGFR3 IIIb were grown in the absence or presence of FGF1 for 3 days with or without the addition of concentrated media (B) or purified FGFR3 Δ8-10 (C). Graphs represent total cell number after 3 days of treatment with and without FGF1. D, 5637 cells transduced with either vector (lanes 1 and 3) or FGFR3 Δ8-10 (lanes 2 and 4) were treated with (lanes 3 and 4) and without (lanes 1 and 2) disuccinimidylyl suberate. The blot was probed with the B9 antibody.

after confluence when receptor levels are at their highest and the cells show aspects of differentiation (29).

In other cell types, such as chondrocytes, FGFR3 signaling can inhibit proliferation and modulate aspects of differentiation (30, 31). In urothelial cells, the overall levels of FGFR3 or the relative levels of isoforms may trigger different downstream signaling responses in different situations. Currently, the pathways stimulated by FGFR3 signaling in urothelial cells are not known but, as has been shown for the mitogen-activated protein kinase pathway, responses to transient or sustained activation of the receptor under different conditions may differ (32–34). In light of our finding of modulation of FGFR3 expression under different growth conditions, it will now be important to examine these aspects of FGFR3 signaling and the expression of FGFR ligands by urothelial cells in detail.

Similar to soluble FGFR splice variants described in previous studies (35, 36), FGFR3 Δ8-10 acted as a dominant-negative regulator of endogenous full-length receptor (Fig. 5). Importantly, this seemed to be a normal signaling event that was repressed in cancer cells. The majority of bladder cancer cells express relatively low proportions of FGFR3 Δ8-10 compared with other isoforms (Fig. 6). Previous reports have shown that FGFR3 Δ8-10 binds to FGF1 and FGF2 (22, 23), indicating relaxed ligand-binding specificity compared with FGFR3 IIIb, which mainly binds FGF1. This is presumably due to the loss of the second half of Ig domain III. Thus, the biological effects of expression of this isoform are likely to be influenced by the presence and availability of these ligands. Our preliminary experiments indicate that NHU cells express both FGF1 and FGF2 transcripts (data not shown) although it is not yet clear whether they are secreted. We have shown that FGFR3 Δ8-10 dimerizes in the presence of endogenous FGF, suggesting that FGF may be sequestered by secreted FGFR3 Δ8-10. This is only one mechanism by which FGFR3 Δ8-10 may inhibit FGF1-induced proliferation. Other mechanisms may include secreted FGFR3 Δ8-10 binding to FGFR3 at the membrane and inhibiting full length receptor dimerization.

FGFR3 is mutated in skeletal disorders (11) and in bladder cancer (8, 17, 18, 20). Mutations in FGFR3 result in prolonged or constitutive activation of the receptor (12, 13). As mutations are frequent in bladder cancer and are clonal events that are presumed to confer a selective advantage, it is predicted that mutant FGFR3 acts as an oncogene in the bladder. FGFR3 mutations are most frequently identified in low-stage and low-grade bladder cancers (~80%; refs. 17, 20, 37) and it has been suggested that the presence of mutation could in some way prevent tumor progression. Repression of a dominant-negative regulatory form of FGFR3 may be another mechanism by which FGFR3 signaling is increased in the initial stages of tumor development.

Analysis of FGFR3 isoform levels in bladder cancer cell lines showed an increase in FGFR3 IIIc expression (Fig. 6). The ratio of the FGFR3 IIIc isoform was increased in 52% of cell lines compared with NHU cells. The presence of FGFR3 IIIc would dramatically affect ligand-receptor binding specificity (3) and may allow cancer cells to bind a wide range of ligands. In this study, the bladder cancer cell lines that expressed more than 40% FGFR3 IIIc isoform levels, and for which tumor stage and grade is available, were all from high-grade and high-stage tumors. J82 was derived from a stage pT<sub>3</sub> grade 3 tumor, BFTC909 from a grade 3 tumor, 96-1 from a pT<sub>3</sub> grade 2 to 3 tumor, SW1710 from a grade 3 tumor, and 253J from a pT<sub>4</sub> grade 4 tumor. In contrast, cell lines derived from bladder cancers of lower stage and/or grade (97-7, pT<sub>1</sub> grade 2-3;



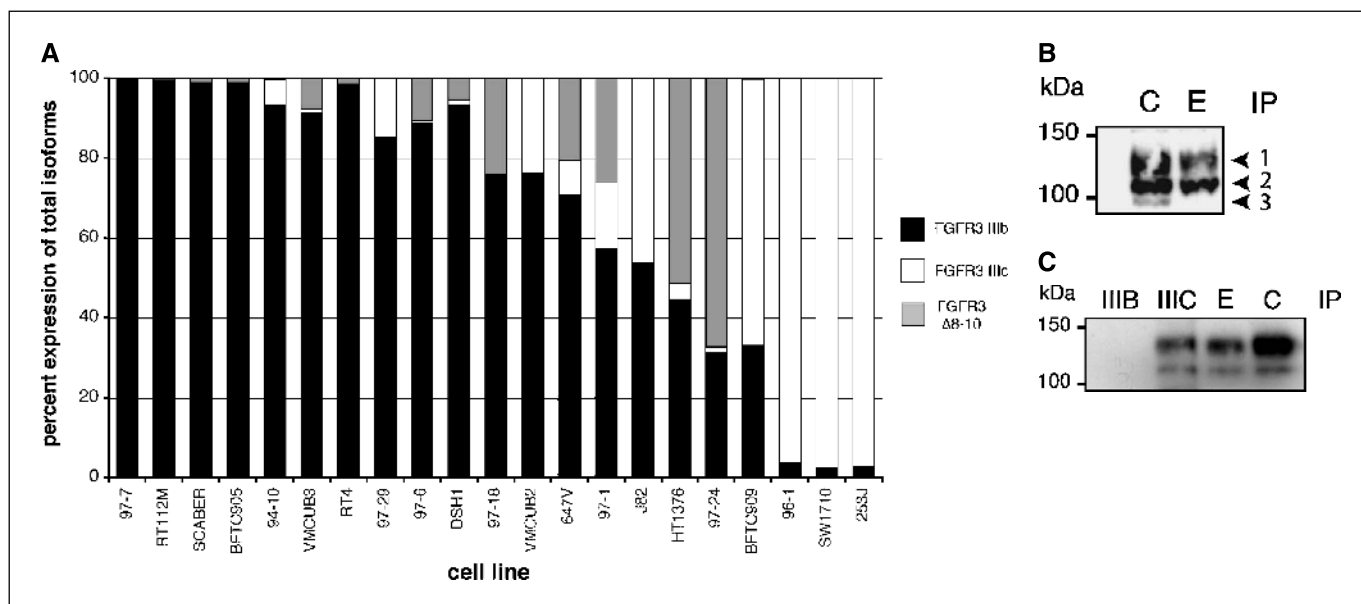


**Figure 6.** Analysis of FGFR3 isoform levels in bladder cancer cell lines. *A*, FGFR3 mRNA levels from 21 bladder cancer cell lines were analyzed by real-time RT-PCR. HPRT was used as an internal control. *B*, 97-7 cell lysates were immunoprecipitated with the FGFR3 C or E antibody and the blot was probed with the B9 antibody. No band 3 was observed in lysates immunoprecipitated with antibody E. *C*, SW1710 cell lysates were immunoprecipitated with the FGFR3 IIIb, IIIc, E, or C antibody and the blot was probed with the B9 antibody. No band was observed in the lysate immunoprecipitation with antibody IIIb.

RT112M, grade 2; RT4, pT<sub>2</sub> grade 1; 97-29, pT<sub>1</sub> grade 1-2; DSH1, pT<sub>1a</sub> grade 2) expressed FGFR3 IIIb as their major transcript. Again, this suggests that FGFR3 IIIb may have tumor-restrictive properties in bladder cancer.

The consensus view that aberrant RNA splicing is a common event during cancer development that may result in a growth advantage for cancer cells has suffered from a lack of data on splicing events in relevant normal cells. Long-term culture of primary normal bladder urothelium has enabled us to examine FGFR3 splicing events in both normal and cancer-derived urothelial cells, a cell type in which FGFR3 clearly plays a role in cancer development. The

finding that FGFR3 Δ8-10 acts as a dominant-negative regulator of FGFR3 signaling and that this isoform may be lost in bladder cancer, where receptor activation by mutation is obviously important, provides us with an impetus to examine further the role of FGFR3 isoforms during cancer progression.

## Acknowledgments

Received 5/19/2005; revised 8/12/2005; accepted 9/12/2005.

The costs of publication of this article were defrayed in part by the payment of page charges. This article must therefore be hereby marked *advertisement* in accordance with 18 U.S.C. Section 1734 solely to indicate this fact.

## References

- Johnson DE, Williams LT. Structural and functional diversity in the FGF receptor multigene family. *Adv Cancer Res* 1993;60:1-41.
- Avivi A, Yayon A, Givol D. A novel form of FGF receptor-3 using an alternative exon in the immunoglobulin domain III. *FEBS Lett* 1993;330:249-52.
- Ornitz DM, Xu J, Colvin JS, et al. Receptor specificity of the fibroblast growth factor family. *J Biol Chem* 1996; 271:15292-7.
- Werner S, Duan DS, de Vries C, et al. Differential splicing in the extracellular region of fibroblast growth factor receptor 1 generates receptor variants with different ligand-binding specificities. *Mol Cell Biol* 1992; 12:82-8.
- Chellaiath AT, McEwen DG, Werner S, Xu J, Ornitz DM. Fibroblast growth factor receptor (FGFR) 3. Alternative splicing in immunoglobulin-like domain III creates a receptor highly specific for acidic FGF/FGF-1. *J Biol Chem* 1994;269:11620-7.
- Morrison RS, Yamaguchi F, Saya H, et al. Basic fibroblast growth factor and fibroblast growth factor receptor I are implicated in the growth of human astrocytomas. *J Neurooncol* 1994;18:207-16.
- Naimi B, Latif A, Fournier G, et al. Down-regulation of (IIIb) and (IIIc) isoforms of fibroblast growth factor receptor 2 (FGFR2) is associated with malignant progression in human prostate. *Prostate* 2002;52: 245-52.
- Cappellen D, De Oliveira C, Ricol D, et al. Frequent activating mutations of FGFR3 in human bladder and cervix carcinomas. *Nat Genet* 1999;23:18-20.
- Luqmani YA, Graham M, Coombes RC. Expression of basic fibroblast growth factor, FGFR1 and FGFR2 in normal and malignant human breast, and comparison with other normal tissues. *Br J Cancer* 1992;66:273-80.
- Fracchiolla NS, Luminari S, Baldini L, et al. FGFR3 gene mutations associated with human skeletal disorders occur rarely in multiple myeloma. *Blood* 1998; 92:2987-9.
- Passos-Bueno MR, Wilcox WR, Jabs EW, et al. Clinical spectrum of fibroblast growth factor receptor mutations. *Hum Mutat* 1999;14:115-25.
- Hart KC, Robertson SC, Donoghue DJ. Identification of tyrosine residues in constitutively activated fibroblast growth factor receptor 3 involved in mitogenesis, Stat activation, and phosphatidylinositol 3-kinase activation. *Mol Biol Cell* 2001;12:931-42.
- Cho JY, Guo C, Torello M, et al. Defective lysosomal targeting of activated fibroblast growth factor receptor 3 in achondroplasia. *Proc Natl Acad Sci U S A* 2004; 101:609-14.
- Webster MK, Donoghue DJ. FGFR activation in skeletal disorders: too much of a good thing. *Trends Genet* 1997;13:178-82.
- Brodie SG, Deng CX. Mouse models orthologous to FGFR3-related skeletal dysplasias. *Pediatr Pathol Mol Med* 2003;22:87-103.
- Chesi M, Brents LA, Ely SA, et al. Activated fibroblast growth factor receptor 3 is an oncogene that contributes to tumor progression in multiple myeloma. *Blood* 2001;97:729-36.
- Billerey C, Chopin D, Aubriot-Lorton MH, et al. Frequent FGFR3 mutations in papillary non-invasive bladder (pTa) tumors. *Am J Pathol* 2001;158: 1955-9.
- Sibley K, Cuthbert-Heavens D, Knowles MA. Loss of heterozygosity at 4p16.3 and mutation of *FGFR3* in transitional cell carcinoma. *Oncogene* 2001;20: 686-91.
- Logie A, Dunois-Larde C, Rosty C, et al. Activating mutations of the tyrosine kinase receptor FGFR3 are associated with benign skin tumors in mice and humans. *Hum Mol Genet* 2005;14:1153-60.
- van Rhijn BW, Lurkin I, Radvanyi F, et al. The fibroblast growth factor receptor 3 (FGFR3) mutation is a strong indicator of superficial bladder cancer with low recurrence rate. *Cancer Res* 2001;61:1265-8.
- Johnston CL, Cox HC, Gomm JJ, Coombes RC.



- Fibroblast growth factor receptors (FGFRs) localize in different cellular compartments. A splice variant of FGFR-3 localizes to the nucleus. *J Biol Chem* 1995;270:30643-50.
22. Terada M, Shimizu A, Sato N, et al. Fibroblast growth factor receptor 3 lacking the Ig IIIb and transmembrane domains secreted from human squamous cell carcinoma DJM-1 binds to FGFRs. *Mol Cell Biol Res Commun* 2001;4:365-73.
23. Jang JH. Identification and characterization of soluble isoform of fibroblast growth factor receptor 3 in human SaOS-2 osteosarcoma cells. *Biochem Biophys Res Commun* 2002;292:378-82.
24. Jang JH, Shin KH, Park YJ, et al. Novel transcripts of fibroblast growth factor receptor 3 reveal aberrant splicing and activation of cryptic splice sequences in colorectal cancer. *Cancer Res* 2000;60:4049-52.
25. Sturla LM, Merrick AE, Burchill SA. FGFR3IIIIS: a novel soluble FGFR3 spliced variant that modulates growth is frequently expressed in tumour cells. *Br J Cancer* 2003;89:1276-84.
26. Shimizu A, Tada K, Shukunami C, et al. A novel alternatively spliced fibroblast growth factor receptor 3 isoform lacking the acid box domain is expressed during chondrogenic differentiation of ATDC5 cells. *J Biol Chem* 2001;276:11031-40.
27. Southgate J, Hutton KA, Thomas DF, Trejdosiewicz LK. Normal human urothelial cells *in vitro*: proliferation and induction of stratification. *Lab Invest* 1994;71:583-94.
28. Sahni M, Ambrosetti DC, Mansukhani A, et al. FGF signaling inhibits chondrocyte proliferation and regulates bone development through the STAT-1 pathway. *Genes Dev* 1999;13:1361-6.
29. Kanai M, Rosenberg I, Podolsky DK. Cytokine regulation of fibroblast growth factor receptor 3 IIIb in intestinal epithelial cells. *Am J Physiol* 1997;272:G885-93.
30. Legeai-Mallet L, Benoist-Lassel C, Delezoide AL, Munnich A, Bonaventure J. Fibroblast growth factor receptor 3 mutations promote apoptosis but do not alter chondrocyte proliferation in thanatophoric dysplasia. *J Biol Chem* 1998;273:13007-14.
31. Dailey L, Laplantine E, Priore R, Basilico C. A network of transcriptional and signaling events is activated by FGF to induce chondrocyte growth arrest and differentiation. *J Cell Biol* 2003;161:1053-66.
32. Pumiglia KM, Decker SJ. Cell cycle arrest mediated by the MEK/mitogen-activated protein kinase pathway. *Proc Natl Acad Sci U S A* 1997;94:448-52.
33. Woods D, Parry D, Cherwinski H, et al. Raf-induced proliferation or cell cycle arrest is determined by the level of Raf activity with arrest mediated by p21Cip1. *Mol Cell Biol* 1997;17:5598-611.
34. Sewing A, Wiseman B, Lloyd AC, Land H. High-intensity Raf signal causes cell cycle arrest mediated by p21Cip1. *Mol Cell Biol* 1997;17:5588-97.
35. Ezzat S, Zheng L, Yu S, Asa SL. A soluble dominant negative fibroblast growth factor receptor 4 isoform in human MCF-7 breast cancer cells. *Biochem Biophys Res Commun* 2001;287:60-5.
36. Celli G, LaRochelle WJ, Mackem S, Sharp R, Merlino G. Soluble dominant negative receptor uncovers essential roles for fibroblast growth factors in multi-organ induction and patterning. *EMBO J* 1998;17:1642-55.
37. van Rhijn BW, Montironi R, Zwarthoff EC, Jobsis AC, van der Kwast TH. Frequent FGFR3 mutations in urothelial papilloma. *J Pathol* 2002;198:245-51.

# Cancer Research

The Journal of Cancer Research (1916–1930) | The American Journal of Cancer (1931–1940)

## Alternative Splicing of Fibroblast Growth Factor Receptor 3 Produces a Secreted Isoform That Inhibits Fibroblast Growth Factor –Induced Proliferation and Is Repressed in Urothelial Carcinoma Cell Lines

Darren C. Tomlinson, Corine G. L'Hôte, Wendy Kennedy, et al.

*Cancer Res* 2005;65:10441-10449.

**Updated version** Access the most recent version of this article at:  
<http://cancerres.aacrjournals.org/content/65/22/10441>

**Cited articles** This article cites 36 articles, 18 of which you can access for free at:  
<http://cancerres.aacrjournals.org/content/65/22/10441.full#ref-list-1>

**Citing articles** This article has been cited by 6 HighWire-hosted articles. Access the articles at:  
<http://cancerres.aacrjournals.org/content/65/22/10441.full#related-urls>

**E-mail alerts** [Sign up to receive free email-alerts](#) related to this article or journal.

**Reprints and Subscriptions** To order reprints of this article or to subscribe to the journal, contact the AACR Publications Department at [pubs@aacr.org](mailto:pubs@aacr.org).

**Permissions** To request permission to re-use all or part of this article, use this link  
<http://cancerres.aacrjournals.org/content/65/22/10441>.  
Click on "Request Permissions" which will take you to the Copyright Clearance Center's (CCC) Rightslink site.